Int. J. Electrochem. Sci., 16**(2021)** Article Number: 211029, doi: 10.20964/2021.10.31

International Journal of ELECTROCHEMICAL SCIENCE
www.electrochemsci.org

Electrochemical sensors based on Au-PPy NPs@f-CNTs nanocomposite modified glassy carbon electrode for determination of Vitamin B12 as a key agent in human motion coordination

Li Guo[1], *Zongyou Yang*[2,*]

[1]School of Physical Education, Southwest University, Chongqing, 400715, China
[2]Department of Physical Education, Chongqing Jiaotong University, Chongqing, 400074, China
[*]E-mail: yangzy888999@163.com

Received: 2 June 2021/ *Accepted:* 30 July 2021 / *Published:* 10 September 2021

This study was focused on the fabrication of electrochemical sensors based on a nanocomposite of Au and polypyrrole nanoparticles and functionalized carbon nanotubes (Au-PPyNPs@f-CNTs) modified glassy carbon electrode (GCE) for detection of Vitamin B_{12} (VB_{12}) content in pharmaceutical and human plasma samples for diagnosis of metabolic disease as a major reason in human motion coordination. The Au-PPyNPs@f-CNTs nanocomposite was chemically synthesized and modified the glassy carbon electrode surface. Structural analyses using SEM and XRD showed that the nanocomposite consisted of deposited Au NPs in fcc crystal structure and amorphous PPy NPs on highly tangled tubes of the f-CNTs network. Electrochemical studies using DPV and amperometry techniques indicted that Au-PPyNPs@f-CNTs/GCE displayed the stable and remarkable electrocatalytic response to additions of VB_{12} due to its high electrical conductivity of Au NPs, PPy NPs and f-CNTs, and well-distributed electrochemically active sites of CNTs. The linear range, limit of detection and sensitivity were obtained 0 to 85 µM, 0.9 nM and 4.3597 µA/ µM, respectively. The applicability of the prepared VB_{12} sensor was investigated in a prepared real pharmaceutical sample of VB_{12} capsules and human plasma samples. Results showed the appropriate accuracy of the analytical results with acceptable recovery and RSD values, indicating the proposed sensor could be reliable for the detection of VB_{12} content in pharmaceutical and human plasma samples for diagnosis of metabolic disease.

Keywords: Au-PPyNPs@f-CNTs; Nanocomposite; Vitamin B_{12}; Human plasma sample; Pharmaceutical sample; Amperometry

1. INTRODUCTION

Coordination disorders often result from malfunction of the cerebellum, the part of the brain that coordinates voluntary movements and controls balance. Dysmetria as a coordination disorder is

the incapability to control the distance, range, and speed of motion required to perform easily coordinated movements [1, 2]. Dysmetria is a signal of cerebellar damage and often presents along with additional signs, for example, loss of poor and balance coordination of walking, eye, and speech movements [3]. More specially, dysmetria is a kind of cerebellar ataxia, which is the common term used to explain abnormal coordination of movements.

Cerebellar damage can result from a variety of causes, including, infection of the brain, stroke, brain tumors cerebral palsy, traumatic brain injury, autoimmune disorders and disorders, demyelinating hereditary degenerative conditions of the nervous system, or metabolic diseases which result of thiamine or vitamin B_{12} deficiency [4-6]. Vitamin B_{12} ($C_{63}H_{88}CoN_{14}O_{14}P$), also known as cobalamin or cyanocobalamin is a cobalt-containing coordination compound that it is important in the normal functioning of the nervous system and in the maturation of red blood cells in the bone marrow.

Thus, the determination of vitamin B_{12} level is important in human plasma, urine, foods and pharmaceutical products for diagnosis and treatment of metabolic disease, and many studies have been focused on chromatography, high-performance liquid chromatography, fluorescence quenching method, fluorimetry, spectrophotometry, electroluminescence, mass spectrometry, atomic absorption spectroscopy, capillary electrophoresis and electrochemical techniques [7, 8]. Among them, electrochemical techniques provide inexpensive strategies for the simple and rapid detection of vitamins, amino acids, minerals and enzymes [9-13]. Modification of the electrode in electrochemical systems by nanostructures hybrid nanocomposites improves sensitivity and stability [14-16]. Therefore, this study was conducted on the fabrication of electrochemical sensors based on Au-PPyNPs@f-CNTs/GCE for detection of VB_{12} contenting in pharmaceutical samples.

2. MATERIALS AND METHOD

2.1. Preparation the modified electrode

For the synthesis of Au NPs [17], The precursor 5 ml of 10mM $HAuCl_4$ (≥99.9%, Sigma-Aldrich) solution was ultrasonically added to 1 ml L-cysteine hydrochloride monohydrate (99%, Haihang Industry Co., Ltd., China), and1 ml cysteamine (99%, Shandong Zhonglan Chemical Co., Ltd., China) aqueous solution. After 20 minutes of ultrasonication, 1 ml of 10mM $NaBH_4$ (99%, Merck, Germany) aqueous solution was gradually added to the solution at room temperature, and the resulted mixture was left to react for 120 minutes. For the preparation of the Au-PPy NPs[18], 6 g polyvinyl alcohol (99%, Hejian Anjiefa Building Material Co., Ltd., China) was mixed with the solution under magnetic stirring for 30 minutes. The mass ratio of Au NPs and PPy NPs was fixed at 1:1. Next, 3 g $FeCl_3$ (≥99%, Merck, Germany) was added to the product under magnetic stirring at 6°C which initiated the polymerization reaction. After 12 hours, the sediments were separated from the liquid phase by filtering (Polycarbonate membrane, 0.2μm, Whatman) and rinsed with deionized water. The as-synthesized Au-PPy NPs were ultrasonically dispersed in ethanol.

To prepare the f-CNTs, CNTs (≥99%, Sigma-Aldrich) was refluxed overnight at 90 °C in 3 M HNO_3 (99.5%, Sigma-Aldrich) that it conducted to side-wall mild oxidation and functionalization of

CNTs [19]. Then, the treated CNTs were filtered and ultrasonically washed and dried. Then, the f-CNTs were ultrasonically dispersed in ethanol and added to disperse Au-PPy NPs suspension. After then, the resulted mixture was dropped on GCE and dried to form the Au-PPyNPs@f-CNTs nanocomposite film. The mass ratio of Au-PPy NPs and f-CNTs were fixed at 3:2.

2.2. Preparation of real samples

The first real sample was prepared from a pharmaceutical sample. VB_{12} capsules were provided from a local pharmacy that was labeled with an amount of 50 µg VB_{12} per capsule. 10 capsules (500µg VB_{12}) were ultrasonically dissolved in50 ml of 0.1 M phosphate buffer solutions (PBS) which were used as a real sample in an electrochemical study through amperometry technique.

The second real sample was prepared from a human blood plasma sample. The VB_{12}-negative plasma sample of a middle-aged man was provided from Beijing Jishuitan Hospital (Beijing, China). 1 mL of samples was diluted to 10mL with the 0.1 M PBS pH 7. The standard addition method was also applied through spike certain concentrations of VB_{12} in the prepared real samples. The spiked samples were stored in the refrigerator at 4 C°.

2.3. Electrochemical and structural Characterizations

DPV and amperometry experiments were conducted on AUTO LAB Potentiostat PGSTAT 302 (Eco Chemie, Utrecht, and The Netherlands) in three-electrode electrochemical set-up containing an Ag/AgCl (saturated KCl) as the reference electrode, a Pt plate as the counter electrode and unmodified and modified GCE as working electrode. The electrochemical electrolyte was 0.1 M PBS which was prepared from an equal volume ratio of 0.1 M NaH_2PO_4 (99%, Sigma-Aldrich) and 0.1 M Na_2HPO_4 (99.95%, Sigma-Aldrich).

The crystal structure and surface morphology of modified electrodes were analyzed through scanning electron microscopy (Hitachi S-4800, Hitachi Ltd., Tokyo, Japan) and X-ray diffraction (XRD, RigakuMiniflex 600, Tokyo, Japan), respectively.

3. RESULTS AND DISCUSSION

3.1. Study the structure and surface morphology

Figure 1 shows the SEM images of f-CNTs/GCE and Au-PPyNPs@f-CNTs/GCE. SEM image of f-CNTs film in Figure 1a displays a network structure of highly tangled tubes with diameters of 50–100 nm which is distributed over the GCE during the drop casting process. It was observed from Figure 1b that Au-PPyNPs@f-CNTs nanocomposite consisted of deposited Au-PPy NPs on the f-CNTs network. Due to rich functional groups of the f-CNTs, the Au-PPy NPs are adsorbed on the surface of CNTs through chemical complex interaction. As observed, the surface of Au-PPy NPs is

smooth, indicating the PPy layer covers pure Au NPs. The average diameter of Au-PPy NPs is 75 nm. The f-CNTs film provided a substrate for the successful formation of porous nanocomposite of Au-PPy NPs on the GCE surface. The highly porous nanocomposite could provide good electron conductivity and shortens ion diffusion path and decrease the ionic diffusion resistance [20-22]. The formation of more active sites on Au-PPyNPs@f-CNTs/GCE can enhance the electrocatalytic activity. Furthermore, the polymer matrix facilitates the effective load transfer from a polymer matrix to CNTs [23].

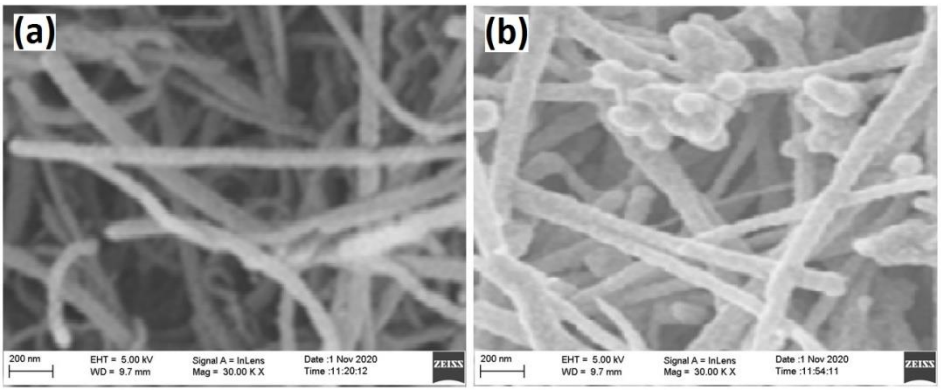

Figure 1. SEM images of (a) f-CNTs/GCE, (b) Au-PPyNPs@f-CNTs/GCE.

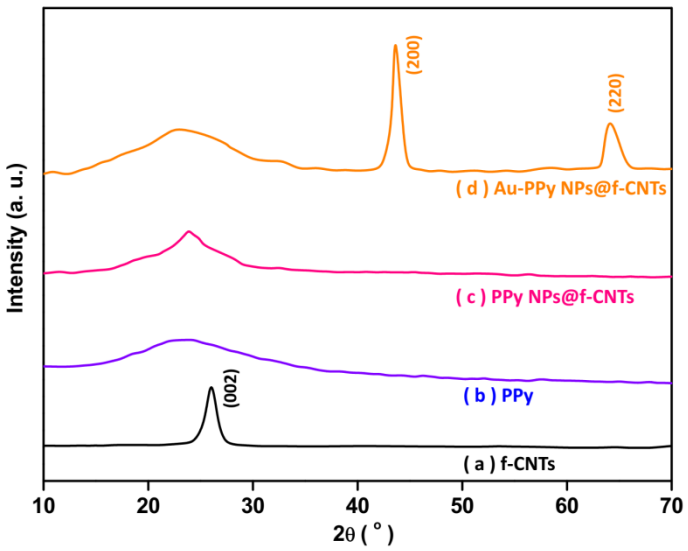

Figure 2. XRD patterns of powders of (a) f-CNTs, (b) PPy, (c) PPyNPs@f-CNTs and (d) Au-PPyNPs@f-CNTs films.

Figure 2 shows the results of the crystal structure of powders of f-CNTs, PPy, PPyNPs@f-CNTs and Au-PPyNPs@f-CNTs films. As seen from Figure 2a, the XRD pattern of the f-CNTs depicts a sharp diffraction peak at 26.30∘, which is corresponding to (002) crystallographic plane off-

CNTs (JCPDS card no. 41-1487) [24]. Figure 2b shows the XRD pattern of PPy with the broad diffraction peak at 2θ=22.85∘ which characteristic of amorphous PPy because of the scattering from PPy chains at the interplanar spacing [25]. Figure 2c displays the XRD pattern of PPyNPs@f-CNTs that it reveals the broad diffraction peak at 23.01°, indicating to f-CNTs embedded into the amorphous PPy matrix. Figure 2d shows the XRD pattern of Au-PPyNPs@f-CNTs nanocomposite with a broad peak at 22.98° which demonstrates the amorphous nature of PPy and the strong peaks at 43.64° and 64.29° assigns to the (200) and (220) planes of face-centered cubic (fcc) structure of Au NPs (JCPDS card no. 04-0784) [26].

3.2. Electrochemical study

Electrochemical responses of the prepared electrodes in absent and additions of 5µM and 10µM VB_{12} solutions were studied using the DPV technique in 0.1M PBS pH 7 at 10 mV/s scan rate.

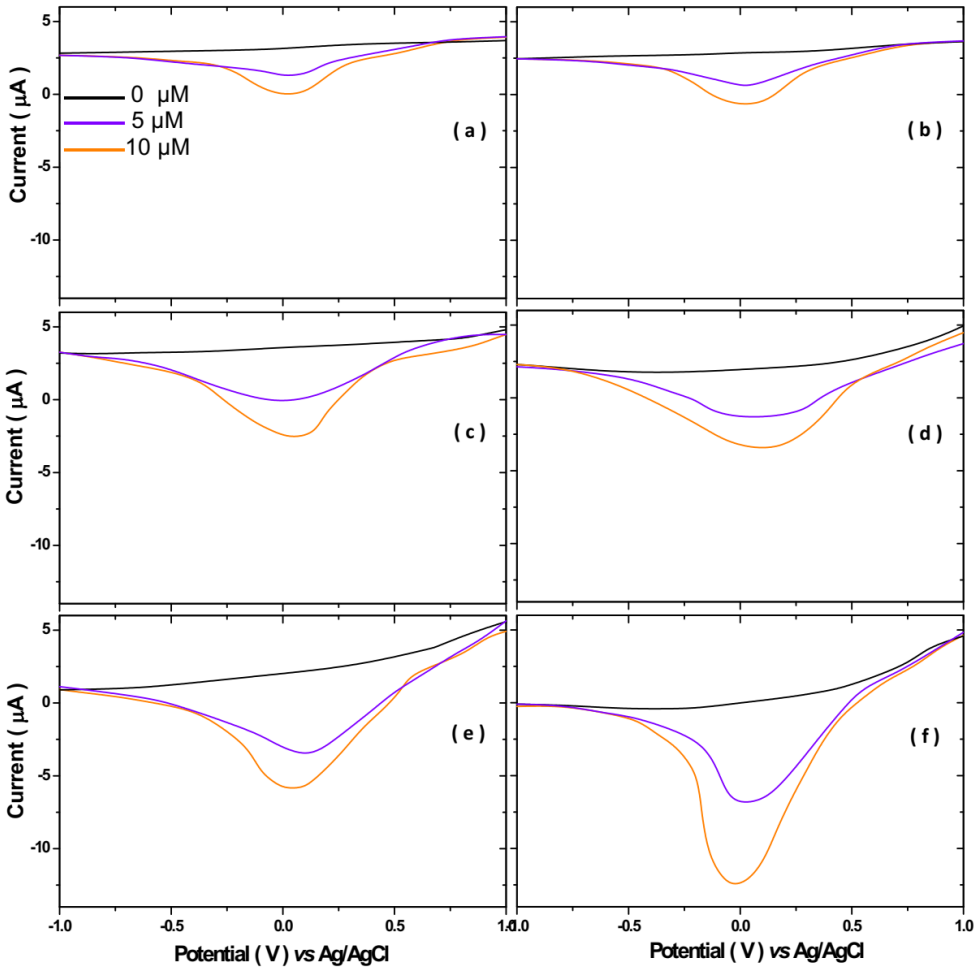

Figure 3. DPV curves of (a) GCE, (b) PPy/GCE, (c) f-CNTs/GCE, (d) PPyNPs@f-CNTs/GCE,(e) Au NPs@f-CNTs/GCE and (f) Au-PPyNPs@f-CNTs/GCE in 0.1 M PBS pH 7 at 10 mV/s scan rate in absent and additions of 5 µM and 10 µM VB_{12} solutions.

Figure 3 show DPV curves of GCE, PPy/GCE, f-CNTs/GCE, PPyNPs@f-CNTs/GCE, Au NPs@f-CNTs/GCE and Au-PPyNPs@f-CNTs/GCE with the reduction peak of VB_{12} at 0.08, 0.06, 0.08, 0.1, 0.04 and -0.02 V, respectively, illustrating to the reduction of the Co(III) center in vitamin B_{12} to Co(I) [27]. Comparison between the DPV curves of GCE, PPy/GCE, f-CNTs/GCE and PPyNPs@f-CNTs/GCE reveals that the f-CNTs play an important role to enhance the electrochemical peak current because of its the functional groups on ends and sidewalls for promoting electron transfer called electron shuttles, the large specific area which providing high sensitivity[28, 29]. In addition, PPy play a leading role due to the relative low redox potential, high stability and great electrical properties [30]. CNTs can also enhance the mechanical strength of PPyNPs@CNTs and Au-PPyNPs@f-CNTs/GCE nanocomposites by serving as structural-reinforcing agents [31]. The lower peak potential and remarkable electrocatalytic response is observed on Au-PPyNPs@f-CNTs/GCE due to its high electrical conductivity of Au NPs, PPy NPs and f-CNTs, and well-distributed electrochemically active sites of CNTs and Au-PPy NPs for the VB_{12} reduction that it can improve the electron-transfer kinetics between the redox active centers of electrode and the electrolyte ions [32, 33]. According the SEM results, the highly porous nonocomposite decreases ion diffusion path and decrease the ionic diffusion resistance [4]. Moreover, enhanced loading capability of Au NPs with active biomolecules that promotes the recognition ratio and binding affinity [32]. Therefore, the Au-PPyNPs@f-CNTs/GCE was selected for further electrochemical studies.

The further electrochemical investigations were carried out using the amperometry technique to evaluate the sensing properties such as stability, linear range, detection limit, selectivity and precise of Au-PPyNPs@f-CNTs/GCE as VB_{12} sensor. Figure 4aexhibits the amperometric response of Au-PPyNPs@f-CNTs/GCE in 0.1 M PBS pH 7 at -0.02 V after the addition of 20 µMVB_{12} solutions. It is found that the amperometry signal is increased after the addition of VB_{12} solutions and long-term stability is observed over 400 s due to the high chemical and mechanical stability of Au and f-CNTs [34]. Figures 4b and 4c display the resulted amperograms and calibration graphs of Au-PPyNPs@f-CNTs/GCE to successive additions of 5 µM VB_{12} solution in 0.1M PBS pH 7 at -0.02 V, illustrating the fast responses of the proposed electrode to any additions of VB_{12} solution. The calibration graph in Figure 4c shows the linear relationship between the amperometric response and VB_{12} concentration from 0 to 85 µM. Furthermore, the limit of detection and sensitivity are obtained of 0.9nM and 4.3597 µA/ µM a, respectively. Table 1 shows the comparison between the obtained linear range and limit of detection of VB_{12} sensor in this work and the other reported carbon and Au-based sensors. As observed, the detection limit values and sensitivity value of Au-PPyNPs@f-CNTs/GCE is comparable than other sensors. The widest linear range is observed for Au-PPyNPs@f-CNTs/GCE in the present study which is attributed to the higher chemical and mechanical stability and higher electrical conductivity of Au-PPyNPs@f-CNTs.

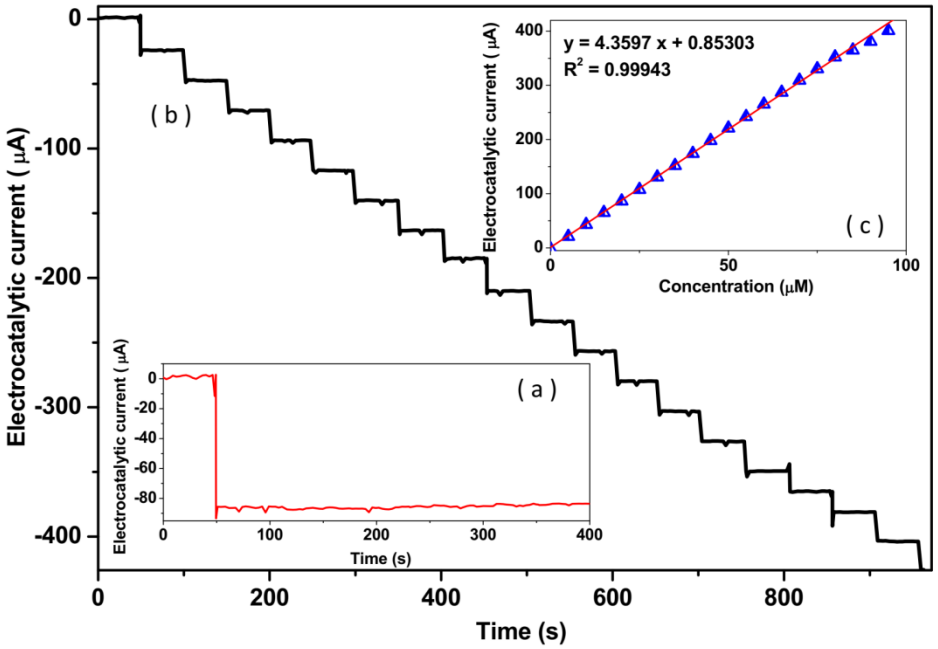

Figure 4. (a) Amperometric response of Au-PPyNPs@f-CNTs/GCE in 0.1 M PBS pH 7 at -0.02 V after addition of 20 µM VB_{12} solution; (b) Amperometric response and (c)calibration graph of Au-PPyNPs@f-CNTs/GCE to successive additions of 5 µM VB_{12} solution in 0.1 M PBS pH 7 at -0.02 V.

Table 1. Comparison between the obtained linear range and limit of detection of VB_{12} sensor in this work and the other reported carbon and Au-based sensors.

Electrode	**Technique**	**Linear Range (µM)**	**limit of detection (nM)**	**Sensitivity (µA/µM)**	**Ref.**
Au-PPyNPs@f-CNTs/GCE	Amperometry	0 – 85	0.9	4.3597	This work
Au–SnO_2 NPs/ITO	DPV	0–0.0015	0.71	-	[35]
Ferromagnetic NPs@itriazinedendrime/ PPy/Au	DPV[c]	0.0025–0.5	0.91	25.6	[36]
SWCNTs/disposable pencil graphite electrode	SWV[d]	0.005–0.1	0.89	1.6	[37]
Poly(2,2′-(1,4-phenylenedivinylene) Bis-8 hydroxyquinaldine)/MWCNTs/GCE	SWV	0.1–10	10	3.726	[38]
Trans-1,2-dibromocyclohexane/carbon paste electrode	SWV	0.002–0.2	0.85	0.014	[39]
Diphenylalanine/pencil graphite electrode	SWV	0.2–9.5	93.0	0.8963	[40]
MWCNTs/GCE	CV	0.1–0.4	1.5	2.885	[41]
Mercaptoacetic acid/ Au	CV	0.04–40	1.0	12.0	[42]

Figure 5 shows the results of the study the repeatability, selectivity and anti-interference capability of Au-PPyNPs@f-CNTs/GCE to determination of VB_{12} through amperometry technique in

0.1 M PBS pH 7 at -0.02 V in successive addition of 1µM VB_{12} solution and 10 µM of K^+, Fe^{3+}, Ca^{2+}, Mg^{2+}, NO_3^- and vitamin D, vitamin B_1, vitamin B_2, vitamin B_6, niacin, folic acid, urea, uric acid, ascorbic acid, and glucose solution as interfering substances. It is observed the electrocatalytic current is significantly increased after first successive additions of 1µM VB_{12} solution (~4.34 µA) and negligible electrocatalytic currents are obtained for addition any interference substances, implying the presented substances do not interfere with the determination of VB_{12} on Au-PPyNPs@f-CNTs/GCE. Moreover, the electrocatalytic current is increased for additions of VB_{12} solution (~4.30 µA) after successive additions of all interference substances that it evidence to stability and repeatability of proposed electrode to the determination of VB_{12}.

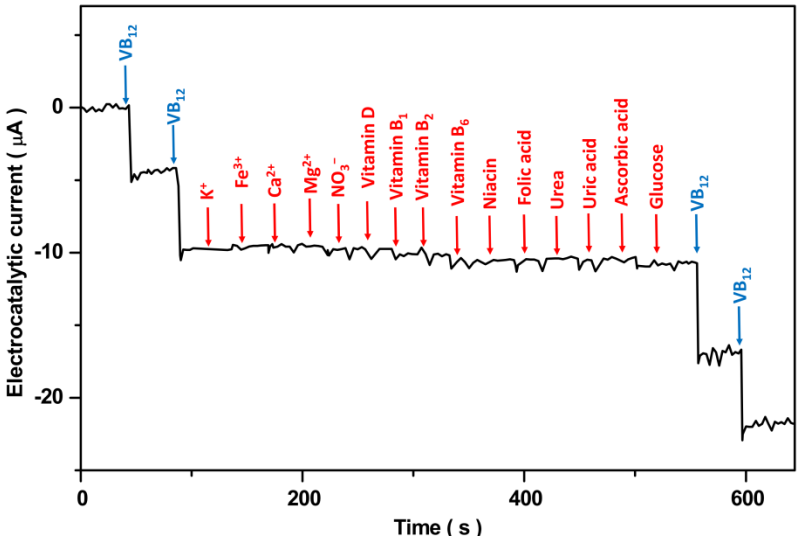

Figure 5. The amperometry response of Au-PPyNPs@f-CNTs/GCE in 0.1 M PBS pH 7 at -0.02V in successive additions of 1 µM VB_{12} solution and 10 µM of interfering substances.

In order to study the applicability of prepared the VB_{12} sensor in a prepared real pharmaceutical sample of VB_{12} capsules, the amperometry experiments was carried out using Au-PPyNPs@f-CNTs/GCE in 0.1 M PBS pH 7 at -0.02 V in successive additions of 1 mg/ml VB_{12} solution. Figure 6a and 6bshow the resulted amperometry response and calibration graph, respectively. The calibration graph illustrates that the VB_{12} concentration in the prepared sample is 0.009 mg/ml that it is very close to the 0.01 mg/ml VB_{12} content, and consequently, it is in agreement with that labeled value of capsules (50 µg per capsule). The analytical applicability of the Au-PPyNPs@f-CNTs/GCE was investigated to determine VB_{12} in the prepared real samples by the standard addition method. It is observed from Table 3 the appropriate accuracy of the analytical results with acceptable recovery values (2.78 to 3.73 %) and relative standard deviation (RSD) values (93 to 98 %). Therefore, the proposed sensor could be reliable for the detection of VB_{12} content in pharmaceutical samples.

The Au-PPyNPs@f-CNTs/GCE capability was also investigated for the determination of VB_{12}in prepared real samples of human plasma through the standard addition method. Amperometry experiments were performed in 0.1 M PBS pH 7 at -0.02 V prepared of real samples. Table 3 shows

the VB_{12}content in real samples and recovery and RSD of spiked levels in human plasma. Results in Table 3 are illustrated that there are no VB_{12} in the sample, and the recovery and RSD values are in the range of 96.40 to 99.32% and 2.71 to 3.48%, respectively, indicating satisfactory and acceptable the precision of performance of Au-PPyNPs@f-CNTs/GCE to the determination of VB_{12} in biological real samples.

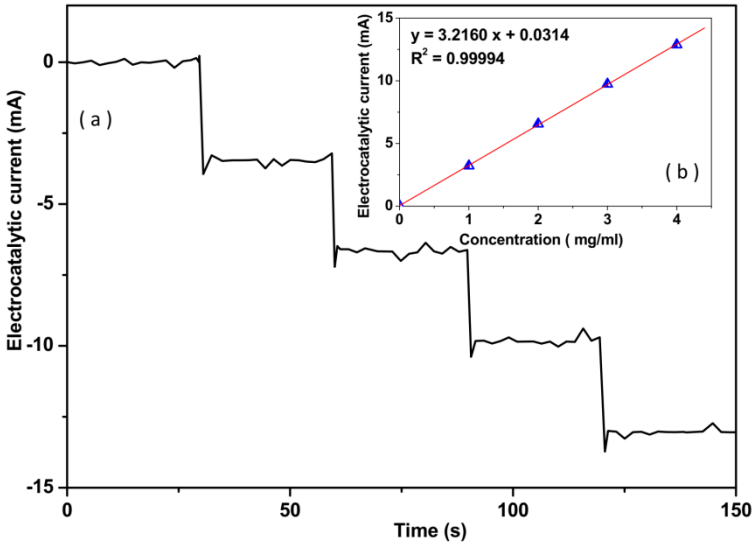

Figures 6. (a) The amperometry response and (b) calibration graph of Au-PPyNPs@f-CNTs/GCE at -0.02 V under successive additions of VB_{12}in prepared 0.1 M PBS pH 7 with real samples.

Table 3. Analytical results of Au-PPyNPs@f-CNTs/GCE to determination VB_{12}in prepared real pharmaceutical and human plasma sample.

Sample	**Added** (mg/ml)	**Found** (mg/ml)	**Recovery (%)**	**RSD (%)**
VB_{12} capsule	0.000	0.009	-	-
	1.000	0.931	93.10	2.78
	2.000	1.942	97.10	3.06
	3.000	2.905	96.83	2.85
	4.000	3.922	98.05	3.73
Human plasma	0.000	0.000	-	-
	1.000	0.966	96.60	3.21
	2.000	1.944	97.20	2.71
	3.000	2.892	96.40	3.12
	4.000	3.973	99.32	3.48

4. CONCULUSION

This work was conducted on the fabrication of electrochemical sensors based on Au-PPyNPs@f-CNTs nanocomposite modified GCE for detection of VB_{12} content in pharmaceutical and human plasma samples for diagnosis of metabolic disease. The nanocomposite was chemically synthesized on the GCE surface. Structural analyses of nanocomposite showed that it consisted of deposited Au NPs and PPy NPs on highly tangled tubes of the f-CNTs network. Results of electrochemical studies showed that Au-PPyNPs@f-CNTs/GCE displayed a stable and considerable electrocatalytic response to additions of VB_{12}. The linear range, limit of detection and sensitivity were obtained 0 to 85µM, 0.9nM and 4.3597µA/µM, respectively. The applicability of prepared the VB_{12} sensor was studied in the prepared real pharmaceutical sample of VB_{12} capsules and human plasma sample. Results showed the appropriate accuracy of the analytical results with acceptable recovery and RSD values, indicating the proposed sensor could be reliable for the detection of VB_{12} content in pharmaceutical samples and biological samples for the diagnosis of metabolic disease.

References

1. M. Manto, *Journal of neuroengineering and rehabilitation*, 6 (2009) 1.
2. Y. Orooji, B. Tanhaei, A. Ayati, S.H. Tabrizi, M. Alizadeh, F.F. Bamoharram, F. Karimi, S. Salmanpour, J. Rouhi and S. Afshar, *Chemosphere*, 281 (2021) 130795.
3. H. Karimi-Maleh, M.L. Yola, N. Atar, Y. Orooji, F. Karimi, P.S. Kumar, J. Rouhi and M. Baghayeri, *Journal of colloid and interface science*, 592 (2021) 174.
4. B. MacDonald, O. Cockerell, J. Sander and S. Shorvon, *Brain*, 123 (2000) 665.
5. L. Mayfrank and U. Thoden, *Journal of neurology*, 233 (1986) 145.
6. H. Karimi-Maleh, S. Ranjbari, B. Tanhaei, A. Ayati, Y. Orooji, M. Alizadeh, F. Karimi, S. Salmanpour, J. Rouhi and M. Sillanpää, *Environmental Research*, 195 (2021) 110809.
7. O. Karmi, A. Zayed, S. Baraghethi, M. Qadi and R. Ghanem, *IIOAB Journal*, 2 (2011) 23.
8. H. Karimi-Maleh, Y. Orooji, F. Karimi, M. Alizadeh, M. Baghayeri, J. Rouhi, S. Tajik, H. Beitollahi, S. Agarwal and V.K. Gupta, *Biosensors and Bioelectronics*, 184 (2021) 113252.
9. J.R. Esch, J.R. Friend and J.K. Kariuki, *International Journal of Electrochemical Science*, 5 (2010) 1464.
10. K. Men, Y. Chen, J. Liu and D. Wei, *International Journal of Electrochemical Science*, 12 (2017) 9555.
11. C. Chen, J. Huo, J. Yin, Y. Li, H. Mao, Q. Zhuo and X. Jia, *International Journal of Electrochemical Science*, 15 (2020) 5262.
12. H. Sadeghi, S.-A. Shahidi, S.N. Raeisi, A. Ghorbani-HasanSaraei and F. Karimi, *International Journal of Electrochemical Science*, 15 (2020) 10488.
13. R. Savari, S. Soltanian, A. Noorbakhsh, A. Salimi, M. Najafi and P. Servati, *Sensors and Actuators B: Chemical*, 176 (2013) 335.
14. H. Savaloni, R. Savari and S. Abbasi, *Current Applied Physics*, 18 (2018) 869.
15. V.D.N. Bezzon, T.L.A. Montanheiro, B.R.C. de Menezes, R.G. Ribas, V.A.N. Righetti, K.F. Rodrigues and G.P. Thim, *Advances in Materials Science and Engineering*, 2019 (2019) 4293073.
16. R. Savari, H. Savaloni, S. Abbasi and F. Placido, *Sensors and Actuators B: Chemical*, 266 (2018) 620.

17. G. Ruggeri, V.L. Covolan, M. Bernabò, L.M. Li, L.F. Valadares, C.A. Leite and F. Galembeck, *Journal of the Brazilian Chemical Society*, 24 (2013) 191.
18. M. Šetka, F.A. Bahos, D. Matatagui, M. Potoček, Z. Kral, J. Drbohlavová, I. Gràcia and S. Vallejos, *Sensors and Actuators B: Chemical*, 304 (2020) 127337.
19. P.-X. Hou, Q. Yang, C. Liu and H.-M. Cheng, *Carbon*, 40 (2002) 81.
20. B. Ding, X. Lu, C. Yuan, S. Yang, Y. Han, X. Zhang and Q. Che, *Electrochimica Acta*, 62 (2012) 132.
21. H. Savaloni, E. Khani, R. Savari, F. Chahshouri and F. Placido, *Applied Physics A*, 127 (2021) 1.
22. F. Chahshouri, H. Savaloni, E. Khani and R. Savari, *Journal of Micromechanics and Microengineering*, 30 (2020) 075001.
23. Y. Zare and K.Y. Rhee, *RSC advances*, 8 (2018) 30986.
24. G. Grassi, A. Scala, A. Piperno, D. Iannazzo, M. Lanza, C. Milone, A. Pistone and S. Galvagno, *Chemical Communications*, 48 (2012) 6836.
25. C. MA, P. SG, G. PR and S. Shashwati, *Soft nanoscience letters*, 2011 (2011) 6.
26. L. Cheng, X. Li and J. Dong, *Journal of Materials Chemistry C*, 3 (2015) 6334.
27. A. Michopoulos, A.B. Florou and M.I. Prodromidis, *Electroanalysis*, 27 (2015) 1876.
28. B. Cardenas-Benitez, I. Djordjevic, S. Hosseini, M.J. Madou and S.O. Martinez-Chapa, *Journal of The Electrochemical Society*, 165 (2018) B103.
29. M.N. Norizan, M.H. Moklis, S.Z.N. Demon, N.A. Halim, A. Samsuri, I.S. Mohamad, V.F. Knight and N. Abdullah, *RSC Advances*, 10 (2020) 43704.
30. M. Lo, M. Seydou, A. Bensghaïer, R. Pires, D. Gningue-Sall, J.-J. Aaron, Z. Mekhalif, J. Delhalle and M.M. Chehimi, *Sensors*, 20 (2020) 580.
31. J. Parayangattil Jyothibasu, M.-Z. Chen and R.-H. Lee, *ACS omega*, 5 (2020) 6441.
32. S. Mehmood, R. Ciancio, E. Carlino and A.S. Bhatti, *International journal of nanomedicine*, 13 (2018)
33. V.S. Manikandan, B. Adhikari and A. Chen, *Analyst*, 143 (2018) 4537.
34. M. Vafaiee, R. Mohammadpour, M. Vossoughi, E. Asadian, M. Janahmadi and P. Sasanpour, *Frontiers in Bioengineering and Biotechnology*, 8 (2021) 1465.
35. A. Sharma, S. Arya, D. Chauhan, P.R. Solanki, S. Khajuria and A. Khosla, *Journal of Materials Research and Technology*, 9 (2020) 14321.
36. M.H. Parvin, E. Azizi, J. Arjomandi and J.Y. Lee, *Sensors and Actuators B: Chemical*, 261 (2018) 335.
37. F. Kuralay, T. Vural, C. Bayram, E.B. Denkbas and S. Abaci, *Colloids and Surfaces B: Biointerfaces*, 87 (2011) 18.
38. H. Filik, A.A. Avan and S. Aydar, *Food Analytical Methods*, 9 (2016) 2251.
39. P. Tomčik, C.E. Banks, T.J. Davies and R.G. Compton, *Analytical Chemistry*, 76 (2004) 161.
40. B.B. Pala, T. Vural, F. Kuralay, T. Çırak, G. Bolat, S. Abacı and E.B. Denkbaş, *Applied Surface Science*, 303 (2014) 37.
41. W. Xiang, J. Li and Z. Ma, *Chinese Journal of Applied Chemistry*, 24 (2007) 924.
42. N. Yang, Q. Wan and X. Wang, *Electrochimica Acta*, 50 (2005) 2175.